

Phase portrait analysis of super solitary waves and flat top solutions

S. V. Steffy^{a)} and S. S. Ghosh^{b)}

Indian Institute of Geomagnetism, New Panvel, Navi Mumbai 410-218, India

(Received 6 April 2018; accepted 8 May 2018; published online 29 May 2018)

The phase portrait analysis of super solitary waves has revealed a new kind of intermediate solution which defines the boundary between the two types of super solitary waves, viz., Type I and Type II. A Type I super solitary wave is known to be associated with an intermediate double layer while a Type II solution has no such association. The intermediate solution at the boundary has a flat top structure and is called a flat top solitary wave. Its characteristics resemble an amalgamation of a solitary wave and a double layer. It was found that, mathematically, such kinds of structures may emerge due to the presence of an extra nonlinearity. Although they are relatively unfamiliar in the realm of plasma physics, they have much wider applications in other physical systems. *Published by AIP Publishing.* <https://doi.org/10.1063/1.5033503>

I. INTRODUCTION

“Supersolitons” or Super Solitary Waves (SSWs) are a new class of nonlinear coherent structures which are characterized by a bipolar electric field structure with wiggles. Compared to the solitary wave, they have larger amplitudes, widths, and velocities. The existence of such structures in plasma was first proposed by Dubinov and Kolotkov¹ and later it was developed by others assuming different plasma models.^{1–11} Our recent works revealed that, apart from an SSW, there exist other kinds of solitary structures, like the Curve of Inflection (CoI), or the generalized Variable Solitary Wave (gVSW). The Sagdeev pseudopotential of a CoI involves a point of inflection while a gVSW is the most general kind of solution associated with a fluctuating charge separation, along with a secondary increase in the charge separation near its maximum amplitude.¹²

Structures like SSW, CoI, or gVSW are all associated with an extra-large amplitude and eventually emerge out of an RSW through a jump condition, characterized by a sudden shooting up of the amplitude over a very small change of the initial parameters.^{12,13} They may thus, together, be identified as Extra-Nonlinear Solitary Waves (ENLSWs) or Other Solitary Waves (OSWs).¹⁴ Previously, Dubinov and Kolotkov¹ worked in detail on various such extra large amplitude structures where, beside the Sagdeev pseudopotential, they also incorporated a phase portrait analysis to identify their solutions. While the pseudopotential represents the nonlinear wave as a trajectory of the pseudoparticle, its phase portrait analysis in the pseudo-space further helps to identify the true characteristics of the associated nonlinear dynamics. Here, the potential represents the pseudo space while the actual space coordinate, or, alternatively, the generalized coordinate of the steady state solution, plays the role of the pseudo-time. The trajectory of the pseudo particle is then analyzed through its phase portrait. Sagdeev himself used the phase portrait analysis to identify the solitary wave solution associated with the pseudopotential.¹⁵ A phase

portrait analysis has also been routinely used for SSWs by other authors.^{1,4,5,16} In our previous works, we have distinguished two types of SSWs which emerge via two different routes from an RSW, viz., the Type I and Type II transitions, respectively. The first one emerges out of a Double Layer (DL) while the other one is associated with a gVSW without having any intermediate DL solution. In this paper, we have focused on their phase portrait analysis. We have found that, between these two types of transitions, there exists a new kind of solitary structure which combines both the characteristics of a Solitary Wave (SW) and a DL. The structure looks like a square potential instead of the usual bell shaped profile and hence we called it a “Flat Top Solitary Wave (FTSW).” We have found that, for an ideal condition, an FTSW will turn to a Triple Root Structure (TRS) where its maximum amplitude merges with a “point of inflection.”^{17,18} The limitations and ambiguities related to an FTSW have been analyzed in detail vis á vis a TRS or traditional DL. The present work will complement our current understanding of the transition of an RSW to SSW in the parameter space.

The paper is organized as follows: Section II gives the analytical formalism of the Sagdeev pseudopotential for our model (Sec. II A) and the upper and lower bounds of the Mach number for the corresponding solitary wave solution (II B). In Sec. III A, we have explored the phase portrait analysis for the Type I (Sec. III A 1), Type II (Sec. III A 2), and intermediate solution (Sec. III A 3). In Sec. III B, the FTSW has been compared with other traditional or analogous kind of solutions, like DL or TRS, while Sec. III C reviews the existing understanding of similar kinds of solutions in other physical systems. The overall discussion and conclusion have been given in Sec. IV.

II. FORMULATION

A. Sagdeev pseudopotential

The model has considered that the plasma is infinite, homogeneous, collisionless, and unmagnetized, comprising two temperature electrons and warm multi-ions. The ions are considered as fluids and the electrons obey Boltzmann distributions. The Sagdeev pseudopotential is derived as¹²

^{a)}steffystephan28@gmail.com

^{b)}sukti@iigs.iigm.res.in

$$\begin{aligned} \Psi(\Phi) = & - \left[(\mu + \nu\beta) \left\{ \mu \left(\exp \frac{\Phi}{\mu + \nu\beta} - 1 \right) + \frac{\nu}{\beta} \left(\exp \frac{\beta\Phi}{\mu + \nu\beta} - 1 \right) \right\} \right. \\ & + \frac{\alpha_l}{6\sqrt{3}\sigma_l} \left\{ \left[(M + \sqrt{3\sigma_l})^2 - 2\Phi \right]^{\frac{3}{2}} - (M + \sqrt{3\sigma_l})^3 - \left[(M - \sqrt{3\sigma_l})^2 - 2\Phi \right]^{\frac{3}{2}} + (M - \sqrt{3\sigma_l})^3 \right\} \\ & \left. + \frac{\alpha_h}{6\sqrt{3}\sigma_h} \left\{ \left[\left(\frac{M}{\sqrt{Q}} + \sqrt{3\sigma_h} \right)^2 - 2\Phi \right]^{\frac{3}{2}} - \left(\frac{M}{\sqrt{Q}} + \sqrt{3\sigma_h} \right)^3 - \left[\left(\frac{M}{\sqrt{Q}} - \sqrt{3\sigma_h} \right)^2 - 2\Phi \right]^{\frac{3}{2}} + \left(\frac{M}{\sqrt{Q}} - \sqrt{3\sigma_h} \right)^3 \right\} \right], \quad (1) \end{aligned}$$

where μ (ν) and β denote the normalized ambient cooler (warmer) electron densities and the cooler to warmer electron temperature ratio while the ionic parameters consist of α_l (α_h), σ_l (σ_h), and Q ($= \frac{m_l}{m_h}$), representing normalized ambient lighter (heavier) ion densities, normalized lighter (heavier) ion temperatures, and the lighter to heavier ion mass ratio, respectively. The subscripts i, e, l, h, c, and w represent ions, electrons, lighter and heavier ions, and cooler and warmer electrons, respectively, and M is the wave Mach number. To incorporate the contribution of both the electrons, we have defined the effective electron temperature $T_{eff} = \frac{T_{ec}T_{ew}}{\mu T_{ew} + \nu T_{ec}}$, T_{ec} (T_{ew}) being the cooler (warmer) electron temperature, respectively. We have also determined the effective linear ion acoustic speed of the system $c_{isl} = \sqrt{\frac{T_{eff}}{m_{il}}}$, accordingly. The usual normalization scheme has been followed where all the temperatures are normalized by T_{eff} , velocities by c_{isl} , the potential ϕ is normalized by $\frac{T_{eff}}{e}$, space by the effective Debye length, and time by the inverse of the plasma frequency which is determined from the total ambient density n_0 . The set of fluid equations are closed by the equation of state for the pressure. More details of the derivation of the Sagdeev pseudopotential and the normalization of the parameters are given in Ref. 17. In order to obtain the solitary wave solution and to ensure the recurrence of the initial state, $\Psi(\Phi)$ of Eq. (1) must satisfy the following boundary conditions:

$$\Psi(\Phi = 0) = \frac{\partial \Psi}{\partial \Phi} \Big|_0 = 0, \quad (2a)$$

$$\frac{\partial^2 \Psi(0)}{\partial \Phi^2} < 0, \quad (2b)$$

$$\Psi(\Phi_0) = 0, \quad (2c)$$

$$\frac{\partial \Psi(\Phi_0)}{\partial \Phi} \neq 0. \quad (2d)$$

This also implies that, $\Psi(\Phi) < 0$ for $0 < \Phi < \Phi_0$, where Φ_0 is the amplitude of the solitary wave. In case of a DL, there is no recurrence of the initial state. The last boundary condition of Eq. (2) thus modifies to the following:

$$\Psi(\Phi_d) = 0; \quad \frac{\partial \Psi(\Phi_d)}{\partial \Phi} = \Delta n_d = 0, \quad (3)$$

where Φ_d is the amplitude of the DL and Δn_d is the charge separation at Φ_d .

B. Mach number (M) limit

For a linear wave, it is the linear dispersion relation of the wave which determines the regime of the wave propagation and its phase velocity. Analogously, it is the Eq. (2b), which describes the boundary condition for the nonlinear solitary wave, determines the lower limit of the corresponding Mach number. Using Eq. (1) in Eq. (2b), one thus obtains the following inequality:

$$\frac{\alpha_l}{M^2 - 3\sigma_l} + \frac{\alpha_h}{\frac{M^2}{Q} - 3\sigma_h} < 1. \quad (4)$$

Solving Eq. (4) for M , one may quantify the lower limit of the Mach number for given plasma conditions. In the present model, we have considered a plasma which consists of H^+ , with a minority component of He^+ , having $Q = \frac{1}{4}$ and $\alpha_l = 0.9$. We have further assumed that both the ions have an equal temperature, viz., $\sigma_l = \sigma_h = 0.033$. Putting these values in Eq. (4), we obtain the following condition:

$$M_n = 1.011; \quad M \geq M_n, \quad (5)$$

where M_n defines that minimum value of the Mach number which supports solitary wave solutions of our model.

Apart from the aforementioned conditions, viz., Eqs. (2a)–(2d) and Eq. (5), it requires an additional condition for the existence of a compressive ion acoustic solitary wave which is generally known as the energy condition for the solitary wave.^{19,20} The condition arises due to the physical requirement that any number density should be a real quantity. For our warm, multi-ion plasma model, the following is the appropriate energy condition for a solitary wave:

$$\Phi_o < \frac{1}{2} (M - \sqrt{(3\sigma_l)})^2. \quad (6)$$

This condition, together with Eqs. (2c) and (2d), implies that, for its maximum Mach number M_x , the Sagdeev pseudopotential should satisfy the following condition:

$$\Psi \left(\Phi = \frac{1}{2} (M_x - \sqrt{(3\sigma_l)})^2 \right) > 0. \quad (7)$$

This together with Eq. (1) gives

$$\begin{aligned} & \mu \left[\exp \left(\frac{(M_x - \sqrt{3\sigma_l})^2}{2(\mu + \nu\beta)} \right) \right] + \frac{\nu}{\beta} \left[\exp \left(\frac{\beta(M_x - \sqrt{3\sigma_l})^2}{2(\mu + \nu\beta)} \right) \right] \\ & < \left(\mu + \frac{\nu}{\beta} \right) + \alpha_l \left[\frac{(M_x^2 + \sigma_l)}{(\mu + \nu\beta)} - \frac{4M_x^{(3/2)}\sigma_l^{(1/4)}}{3(\mu + \nu\beta)} \right] \\ & + \alpha_h \left[\frac{\left(\frac{M_x^2}{Q} + \sigma_h \right)}{(\mu + \nu\beta)} \right] - \frac{\alpha_h}{6\sqrt{3}\sigma_h(\mu + \nu\beta)} \\ & \times \left[\left\{ \left(\frac{M_x}{\sqrt{Q}} + \sqrt{3\sigma_h} \right)^2 - (M_x - \sqrt{3\sigma_l})^2 \right\}^{3/2} \right. \\ & \left. - \left\{ \left(\frac{M_x}{\sqrt{Q}} - \sqrt{3\sigma_h} \right)^2 - (M_x - \sqrt{3\sigma_l})^2 \right\}^{3/2} \right]. \end{aligned} \tag{8}$$

For appropriate electronic and ionic plasma parameters, this fixes the upper limit of M, beyond which the solitary wave solution ceases to exist and the wave breaks due to the excessive steepening. Both Eqs. (5) and (8), together, determines the corresponding existence domain of the solution.

III. RESULT AND DISCUSSION

A. Phase portrait analysis

It is now well known that the electronic parameters, viz., μ and β , play pivotal roles to determine any ENLSW solution. To find out the adequate range of these parameters supporting SSWs, we have plotted the variation of Φ_x with β in Fig. 1, where Φ_x is the amplitude of the solitary wave at its corresponding maximum Mach number, i.e., $M = M_x$ [Eq. (8), Sec. II B]. For our convenience, we have kept all the ionic parameters constant. In the entire analysis, the cooler electron concentration μ ($= 0.00151$) has also been remained constant. Figure 1 readily reveals two distinct phases, or regions, viz., A and B, where the limiting solutions for A are DLs and that for B are SWs. Phase B is further divided between two subregions, viz., B1 and B2. For both regions A and B1, the amplitude increases with β but for B2, it decreases. The largest amplitude has been attained for the intermediate region B1 which also governs the ENLSWs. This in turn determines the range of β values supporting the

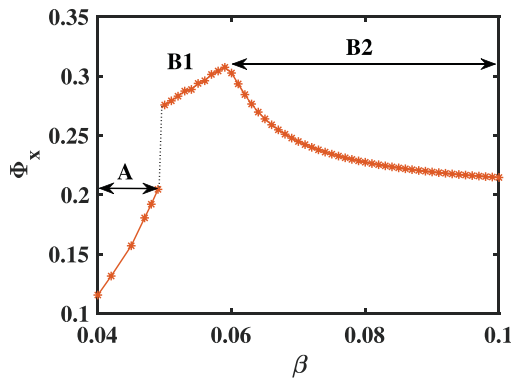


FIG. 1. Variation of Φ_x with β .

said solutions. The onset of B1 is marked by a sudden and discontinuous jump in the amplitude vis á vis region A and it terminates with an abrupt change in its slope.

Figure 1 establishes the range of β supporting ENLSWs, which is determined by region B1. Since SSWs are a subset of ENLSWs, they too are confined by the same range of β . We recall that the SSWs may further be characterized by their process of onset from an RSW, viz., the Type I and Type II transitions, where the latter occurs for a larger value of β . We have chosen two distinct β values from both the lower and upper end of B1 representing Type I and Type II transitions, respectively. For each β , we have varied M to carry out the phase portrait analysis. For each of the cases, the ionic parameters and the cooler electron concentration (μ) remain constant which, along with the fixed value of β , ensures the invariance of the background plasma parameters. The variation of the solution thus solely caused by the variation in the initial perturbations, leading to the present steady state solution.

1. Type I transition

A Type I transition has been defined as one where an RSW transforms to an SSW through an intermediate DL. Figure 2(a) shows a typical set of solutions following Type I transition. The dashed curve (curve 1) represents an RSW and the dashed-dotted curve (curve 3) represents an SSW while the intermediate solid curve (curve 2) is a DL. For the

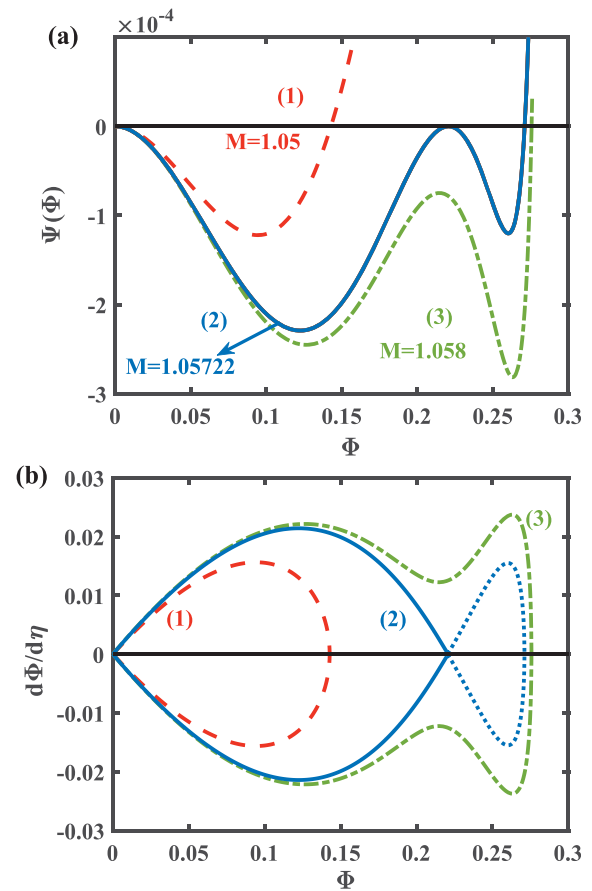


FIG. 2. (a) Sagdeev pseudopotential profiles correspond to Type I transition (1) RSW, (2) DL and (3) SSW and (b) corresponding phase portrait.

current analysis, we have chosen our β ($= 0.05$) at the onset of region B1 and varied the Mach number. Figure 2(b) further represents the corresponding phase portraits. The saddle point of both the inner close curves (dashed) and outer ones (dashed-dotted) at zero ensures solitary wave solutions while the solid curve represents the separatrix associated with the DL. The extension of this solid curve in the phase portrait is shown by the dotted curve [Fig. 2(b)], which is non-physical. The presence of the separatrix indicates differences in the nonlinear dynamical processes involved in an RSW (inner curves) and SSW (outer curves) and justifies the attribute “super” for the latter as it appears beyond the separatrix and engulfs, or envelopes, all the inner curves, including the separatrix. It also shows the “wobble,” or deformations, near the maximum amplitude, which is the hall mark of an SSW solution. Dubinov and Kolotkov² have previously defined an SSW in terms of the separatrix which was further supported by others.^{4,5} The present result thus agrees well with the previous findings.

2. Type II transition

Here, we have considered a β ($\beta = 0.051$) value near the middle part of region B1 and we keep all the other parameters same as before. Figures 3(a) and 3(b) show the respective Sagdeev pseudopotentials and phase portraits for the M variation, respectively, where the dotted curve represents the p-CoI (curve 3), the solid curve represents gVSW (curve 2), and other curves (curves 1 and 4) follow the same

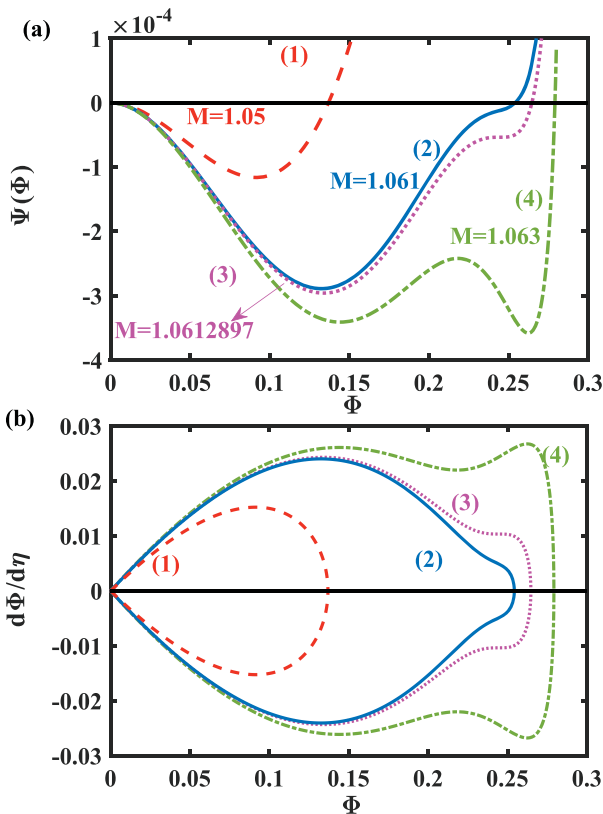


FIG. 3. (a) Sagdeev pseudopotential profiles correspond to Type II transition (1) RSW, (2) gVSW, (3) p-CoI, and (4)SSW and (b) corresponding phase portrait.

as in Fig. 2 legend. The most striking result in Fig. 3(b) is that it has no separatrix. Instead, there is a gradual deformation of the trajectory (curve 2) leading to a fully grown “wobble,” or “fold,” of the SSW (curve 4). In the absence of a separatrix, the attribute “super” loses its significance for the SSW. Instead of a DL, a gVSW (solid curve) initiates the minor deformations which in turn mark the onset of the ENLSW in general. A p-CoI (curve 3) further marks the onset of an SSW beyond the gVSW. This particular transition we have called as Type II which does not involve any DL or separatrix. This may also call for the modification of the definition for an SSW where it may best be defined by its extra fold in the otherwise bipolar electric field (a folded solitary wave or FSW) rather than its “super nonlinearity” beyond the separatrix. While the actual nonlinear dynamical processes may well differ between Type I and Type II, the potential and electric field profiles remain indistinguishable for both the cases.

3. The intermediate solution: FTSW

The previous analyses in Secs. III A 1 and III A 2 ask for the limiting value of β which marks the boundary of these two kinds of transformations. We have found that, for our chosen set of parameters, $\beta = 0.0507$ is that maximum value of β beyond which no Type I transformation occurs. We defined this particular β value as β_r , and explored the corresponding Sagdeev pseudopotentials and phase portraits in Figs. 4(a) and 4(b), respectively. Figure 4(b) recovers the separatrix ensuring a Type I transition. The corresponding solution has been presented by a solid line (curve 2) while other legends remain the same.

Curve 2 immediately raises the question whether it is a DL, due to its association with a separatrix (Type I transition), or a no-DL, since it lacks a local maxima at its maximum amplitude. According to Eq. (3), a DL should have a charge neutral point (i.e., $\Delta n = 0$) at its maximum amplitude. To ascertain this condition, we have incorporated the derivative analysis of curve 2. Figures 5(a) and 5(b) show the variations of the 1st and 2nd derivatives of curve 2 with Φ . Particularly, the former shows a 99% drop from its maximum value giving rise to a charge separation of the order of Δn ($= \frac{\partial \Psi}{\partial \Phi}$) $\approx 10^{-5}$ at Φ_0 while its maximum value lies within the order of 10^{-3} [Fig. 5(a)] for the selected range of Φ , viz., $0 \leq \Phi \leq \Phi_0$. This surely makes the solution DL like, ensuring a separatrix and a Type I solution. However, it also assures a remaining charge separation at the maximum amplitude which is 1% of its maximum value. Figure 5(b) further shows that the 2nd derivative drops to a value of the order of 10^{-4} at its maximum amplitude which is though small compared to its maximum value ($\frac{\partial^2 \Psi}{\partial \Phi^2} \approx 10^{-2}$), yet remains a finite and non-zero positive quantity. With these two values together, the ideal charge neutrality condition at its maximum amplitude for the DL is not satisfied for the said solution. On the other hand, the small but positive non-zero value of its 1st derivative ideally satisfies the condition in Eq. (2) which enables the pseudoparticle to retrace its reflected trajectory fulfilling the recurrence condition.

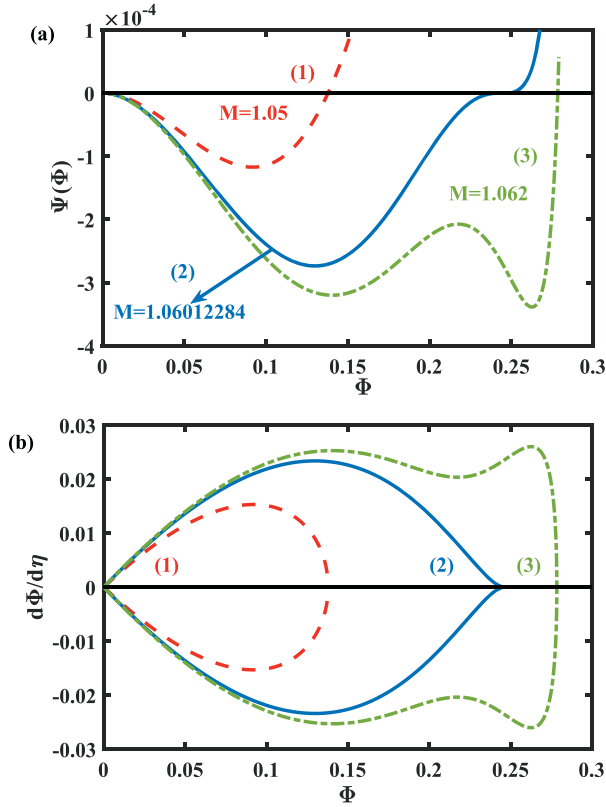


FIG. 4. (a) Sagdeev pseudopotential profiles correspond to the transition at the boundary of Type I and Type II (1) RSW, (2) flat-top solitary wave, and (3) SSW and (b) corresponding phase portrait.

Following the above argument, we have plotted the potential in Fig. 6. The left side of the figure represents the reflected part of the solitary structure. Together, they reveal a Flat Top Solitary Wave (FTSW) whose morphology differs from their usual bell shaped profiles. The solution is a perfect amalgamation of a SW and DL and it represents the intermediate solution between the Type I and Type II SSWs for the chosen set of parameters.

Following Eqs. (2) and (3), we may now find an analogous condition for FTSW which will state that

$$\Psi(\Phi_0) = 0 \quad \frac{\partial \Psi}{\partial \Phi} \Big|_{\Phi_0} = \epsilon \quad \frac{\partial^2 \Psi}{\partial \Phi^2} \Big|_{\Phi_0} = \delta \quad \epsilon, \delta \neq 0, \quad (9)$$

where both ϵ and δ are small and real numbers. To complement our findings, we have also plotted Φ_x and β for region

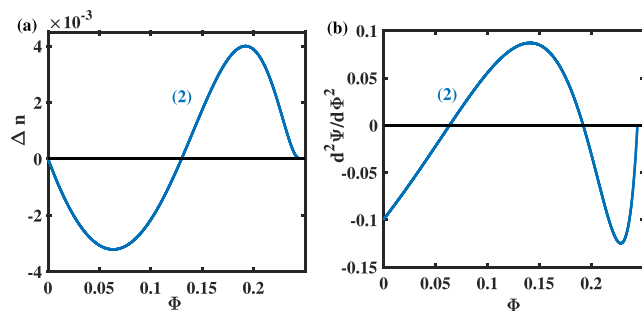


FIG. 5. (a) First derivative of the Sagdeev pseudopotential of an FTSW. (b) Second derivative of the Sagdeev pseudopotential of an FTSW.

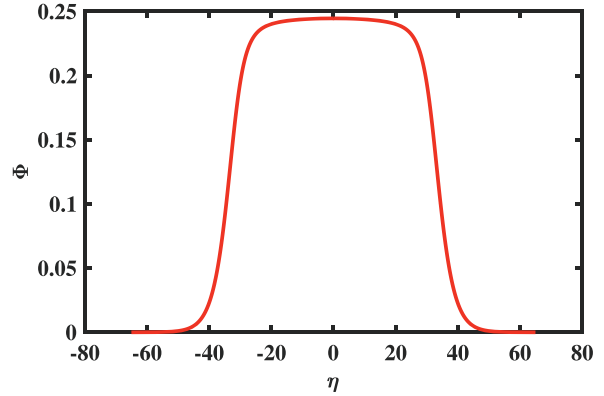


FIG. 6. Potential profile corresponding to an FTSW.

B1 in Fig. 7 which ascertains three subregions, viz., a, b, and c, marked by the dashed lines. The β value associated with the FTSW, namely, $\beta = \beta_r$, determines the boundary between first two subregions, viz., a and b, representing Type I and Type II transitions, respectively, while beyond b, (i.e., subregion c), there is no SSW solution.

B. Comparison between FTSW and DL: Triple Root Structures (TRS)

Arguably, the FTSW solution obtained in Sec. III A 3 needs further attention. For this, it is necessary to revisit a true, or ideal DL solution vis á vis FTSW. Generally, a DL solution obtained by Sagdeev pseudopotential is a numerical approximation of the true or ideal DL. Figure 8(a) highlights the general trend of the pseudopotential around Φ_d , the amplitude of DL. The local maxima ideally satisfies the second part of Eq. (3) ensuring the point of charge neutrality. The trend shown in Fig. 8(a) further ensures the existence of a true DL between curves 1 and 2 for which, ideally, $\Psi(\Phi) = 0$ at $\Phi = \Phi_d$. This is further validated in Fig. 8(b) which shows the variation of Ψ_m with M . Here we have defined Ψ_m as Ψ at its maxima near Φ_d which implies that $\frac{\partial \Psi}{\partial \Phi} = 0$ for each Ψ_m [Fig. 8(b)]. Since the curve crosses the zero axis, it further ensures the existence of a true DL with $\Psi_m = 0$ for certain $M = M_d$ where $1.0572 < M_d < 1.05725$.

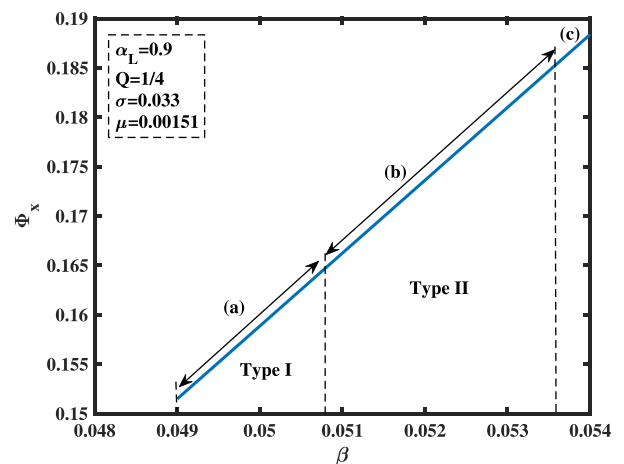


FIG. 7. Variation of Φ_x Vs β for region B1 in Fig. 1.

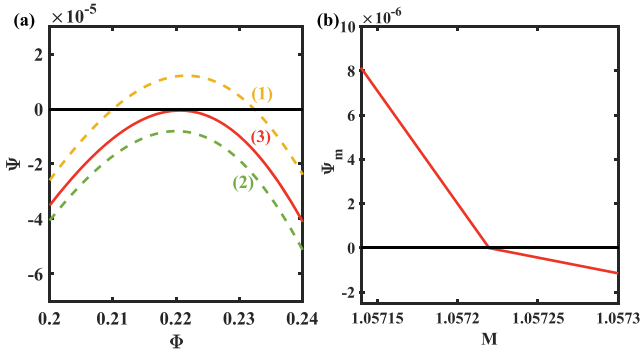


FIG. 8. (a) Trend of Sagdeev pseudopotential around Φ_d and (b) Variation of Ψ value at the peak with M .

We have previously noticed that, for the range of our interest, i.e., $0 \leq \phi \leq \phi_d$, $|\Psi|$ remains within the order of around $< 10^{-4}$ [Fig. 2(a)]. Given that, we have chosen a vanishingly small $|\Psi_m|$, ($|\Psi_m| < 10^{-11}$), as the required DL solution. This provides a reasonable accuracy for the present case within the range of $0 \leq \Phi \leq \Phi_d$. The condition for a true, or ideal DL may thus be modified from Eq. (3) as

$$\Psi(\Phi_d) = \frac{\partial \Psi}{\partial \Phi} \Big|_{\Phi_d} = 0; \quad \frac{\partial^2 \Psi}{\partial \Phi^2} \Big|_{\Phi_d} < 0. \quad (10)$$

So far the last condition for the 2nd derivative was never considered possibly because it was assumed obvious, since the pseudopotential is already a negative, and may also partly because anything beyond Φ_d is supposed to be non-physical. Therefore, Eq. (10) should better be considered as the more complete condition for a true DL.

Recent discoveries of SSW and other associated ENLSWs, like gVSWs and CoIs, establishes the possibility of finding more and more special and composite structures beyond the classical solitary waves. Let us assume a Sagdeev pseudopotential for which its point of inflection coincides with its amplitude. The required condition would then be

$$\Psi(\Phi_0) = \frac{\partial \Psi}{\partial \Phi} \Big|_{\Phi_0} = \frac{\partial^2 \Psi}{\partial \Phi^2} \Big|_{\Phi_0} = 0. \quad (11)$$

Since all the three quantities vanishes at $\Phi = \Phi_0$, they may rightly be called as a Triple Root Structure (TRS). It means that, ideally, the reflection point for the pseudo particle now lies at infinity. Leaving $\Phi = 0$ at rest, it will reach its reflection point after an infinite fictitious time, and then it will again oscillate back to $\Phi = 0$ with an infinitely long time period. In reality, this may well be considered as a DL-like solution with amplitude Φ_r , satisfying Eq. (3), where Φ_r is that first, or minimum value of Φ which ideally satisfies Eq. (3). Beyond Φ_r , everything else will be discarded as non-physical. A TRS solution was first identified by Hellberg *et al.*,¹⁷ and later have been analyzed by Verheest¹⁸ in their recent works.

A comparison between Eqs. (9) and (11) readily reveals that, for $\epsilon \rightarrow 0$, $\delta \rightarrow 0$, an FTSW turns to a TRS. This raises the question whether an FTSW solution can be considered or approximated as a TRS. To resolve this ambiguity, we have

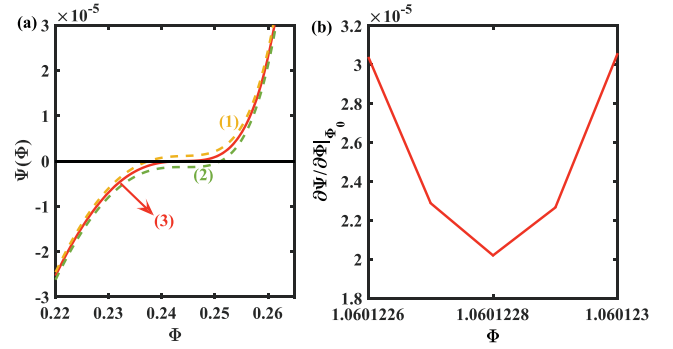


FIG. 9. (a) Trend of the Sagdeev pseudopotential near the amplitude of an FTSW and (b) variation of $\frac{\partial \Psi}{\partial \Phi} \Big|_{\Phi_0}$ with M .

highlighted the trend of the Sagdeev pseudopotential near the maximum amplitude of an FTSW in Fig. 9(a). While it satisfies the first part of the conditions in Eq. (3) and (11), i.e., $\Psi(\Phi_0) = 0$, trivially, the trend in Fig. 9(a) itself does not ensure remaining two conditions for the derivatives. In order to ascertain this, in Fig. 9(b), we have plotted the variation trend of $\frac{\partial \Psi}{\partial \Phi}$ at $\Phi = \Phi_0$ with Mach number (M). From Fig. 9(b), it is well evident that, as M increases, $\frac{\partial \Psi}{\partial \Phi} \Big|_{\Phi_0}$ reaches a minimum value and then it again starts to increase abruptly. This trend strikes out the possibility of obtaining $\frac{\partial \Psi}{\partial \Phi} = 0$ at $\Phi = \Phi_0$. In other words, unlike Fig. 8(b) which represents a true DL, Fig. 9(b) does not ensure the existence of a true TRS satisfying the condition of Eq. (11) ideally. On the contrary, our analyses have indicated that both ϵ and δ are bounded by some minimum value and any minor change in the initial parameters increases their values drastically pushing the solution abruptly away from any possible TRS kind of solution. Conversely, the accuracy for a DL, solution can be increased seamlessly by a fine modulation of any of the parameters which justifies its aforementioned approximation. A similar justification could not be found for the FTSW and hence we opine that it should be considered as a separate kind of solitary wave rather than a TRS solution.

For our current model and analyses, we were unable to find any solution which can be judiciously approximated as a TRS, satisfying the condition of Eq. (11) with a reasonable accuracy. This certainly does not exclude the possibility of finding a TRS in future. We, however, opine that, for any such cases, the accuracy of both ϵ and δ should be taken care of so that the conditions in Eq. (11) can be justified. Otherwise, in spite of its strong DL like properties, the boundary conditions for the solution will still fall in the category of a solitary wave and should better be called as an FTSW rather than a TRS.

C. FTSW in plasma and other fields

It is well known that the solutions of a class of integrable Non-Linear Partial Differential Equations (NLPDEs) exhibit localized nonlinear structures like solitons or DLs. The former has a typical bell shaped profile of sech^2 while the latter has a step like structure with a \tanh profile and often known as the kink soliton. As the subject starts evolving with time, it has become more and more evident that

there exist far richer varieties of integrable and non-integrable NLPDEs, governing many other kinds of organized nonlinear structures which differ significantly from their aforementioned classical counterparts.²¹ Some examples of these new kinds of structures are the forced, or accelerated solitons,^{22,23} dissipative solitons,^{24,25} multi-solitons, or multi-peak solitons,²⁶ breathers, Flat Top Solitons (FTSs),²⁷ and kink-antikink pairs,²⁸ to name a few. They, together, not only opened a new gamut of nonlinearities but also found an wide range of applications in different physical systems, like photonics,^{29,30} nonlinear optics,³¹ lattice dynamics,^{32,33} hydrodynamics,³⁴ acoustics,^{33,35} biophysics,³⁶ chemical physics,³⁷ high energy physics,³⁸ Bose-Einstein condensates,³⁹ cosmology,⁴⁰ metal alloys,⁴¹ and so on. Among all others, particularly, the FTS and the kink-antikink pair are found to have a good resemblance with our own FTSW solution and need a closer look. We have mentioned some of those relevant works in the next sections (Secs. III C 1 and III C 2).

1. Flat top solitons

Flat top solitons are mostly studied in nonlinear optics³¹ and photonics,²⁹ both theoretically and experimentally. Comparatively we could find fewer applications in the plasma physics. They are spatially extended solutions having a flat spatial profile at the center and hence are called Flat Top Solitons. Mathematically, they have been obtained as a special solution of a modified form of the NLPDEs. A few such examples are the extended Korteweg–de Vries (eKdV) equation, nonlinear Schrodinger (NLS) equation, cubic-quintic nonlinear Schrodinger (CQNLS) equation, or Gardner equation. Grimshaw *et al.*⁴² studied the extended version of the K-dV equation (eK-dV) which is different from the usual K-dV equation in having an extra cubic term of nonlinearity. This equation is alternatively called as Gardner equation. This extra nonlinearity leads to many different kind of solutions, including FTS. Specifically, for a large amplitude initial perturbation, the system supports “table top soliton” with a flat centered potential profile, instead of the usual bell shaped one. Later, Tribeche *et al.*²⁷ analyzed the nonlinear Quantum Dust Ion Acoustic (QDIA) solitons by adopting a quantum hydrodynamical model for three species quantum plasma. Under certain parametric conditions, they obtained a broad centered Flat Bottomed Soliton, which is the rarefactive counterpart of an FTS. They, however, interpreted their solution as a kink-antikink pair rather than a soliton. Relativistic electromagnetic FTS solutions have been obtained numerically for a laser pulse propagating through the plasma medium.⁴³ The structures are essentially a large amplitude one, appearing at the boundary of the bright and dark solitons and satisfy charge neutrality conditions at its center.⁴³ FTS solutions obtained from eK-dV or Gardner equation are found to be appropriate in explaining large amplitude internal waves in the ocean.²¹ The study of the FTS has also been extended to a multi-dimensional hydrodynamical system.³⁴ Recently, multi-peak and flat top solitary waves have been presented for an electron-positron-ion (e-p-i) plasma with an implication of laser-plasma interactions.²⁶ Overall, these flat top structures imply

a richer and new kind of nonlinear dynamical behaviors which not only have a strong mathematical foundation but may also have more realistic applications in different physical systems.

It is evident that structurally an FTS is identical with the FTSW obtained from the present Sagdeev pseudopotential analysis. We already know that a soliton is, eventually, an idealized subset of solitary waves where the latter is physically more realistic and need not be bounded by any strict mathematical formalism.⁴⁴ In the same light, an FTSW presented here is a more generalized representation of an FTS which is not associated with any specific NLPDE but represents all its relevant physical characteristics.

2. Kink-antikink pair

In literature, there are many mentions of kink-antikink pairs for different physical systems which includes as diverse topics as phase transitions in metal alloys,⁴¹ high energy physics,³⁸ or biophysics.⁴⁵ Like an FTS, they, too, are obtained from the solutions of NLPDEs.^{28,46,47} Within our present formalism, a kink-antikink pair basically represents the coexistence of two DLs with opposite polarities which are ideally apart by an infinite time duration. Recently, the coexistence of both positive (compressive) and negative (rarefactive) amplitude DLs have been studied in detail by Ali *et al.*⁴⁸ assuming the same Sagdeev pseudopotential technique for an e-p-i plasma.

Unlike the present formalism of the Sagdeev pseudopotential technique, an NLPDE may well possess a multi-soliton solution. A kink-antikink pair is also a class of multi-soliton solution where a kink, or DL, may come back to its initial state through an antikink, thus preserving the net energy of the system. A judicious combination of kink-antikink pair may thus resemble an FTS solution, giving rise to a similar, overall top-hat kind of potential.²⁸ Sometimes an FTS has thus been interpreted as a kink-antikink pair.²⁷ Although there is an apparent similarity between the two, an FTSW should better be interpreted as an amalgamation of an SW and DL, rather than a kink-antikink pair. The structure goes very near to a DL-like solution attaining an almost quasi neutrality condition, but bounces back to its initial state retaining the characteristics of an SW. The prolonged sustentation of a very low charge separation causes the flat and wide central part of the structure which may be associated with a greater degree of dispersion. Results obtained from an eK-dV or Gardner equation⁴² suggests a “secondary insurgence in the nonlinearity” which balances the excessive dispersion maintaining the solitary structure. They may also be visualized as a composite structure vis á vis the usual classical solitary waves which defines the boundary between the two “phases” of SSWs.

IV. CONCLUSION

In this paper, we have presented the phase portrait analysis of the SSWs. It reveals a novel structure with a flat top profile at the boundary of the two types of SSWs. Although they appear to be “new” at its first glance, similar types of profiles have already been identified for a QDIA plasma,²⁷ or

the relativistic laser-plasma interaction.⁴³ The current profile, which we named as an FTSW within the framework of Sagdeev pseudopotential, is nothing but a generalization of already known flat top solitons which, like their classical counterpart, i.e., the regular soliton with a sech^2 profile, emerge as a solution of a class of NLPDEs.

Although the morphology of the potential profile of an FTSW is apparently similar to that for a kink-antikink pair, their boundary conditions differ [Eq. (8)]. An FTSW has a finite time duration and arises due to the reflection of the pseudoparticle which is physically different from a kink-antikink pair. The small but finite $\frac{\partial\Psi}{\partial\Phi}$ ($\approx 10^{-5}$) at its maximum amplitude allows us to consider them as a solitary wave solution rather than a DL. It is to be noted that the current formalism of Sagdeev pseudopotential essentially provide a “single,” “steady state” solution and does not support any multi-soliton structure. However, for an ideal condition where $\frac{\partial\Psi}{\partial\Phi} = 0$ at its maximum amplitude, an FTSW will turn to a TRS which may be interpreted as an infinitely apart pair of kink and antikink.

Although we have rediscovered FTSW during our course of study of SSWs, it appears to have a much richer nonlinear dynamical properties and is fairly interdisciplinary. Appearing as a special class of solutions for the Sagdeev pseudopotential, it also has a robust mathematical foundation by its own. The solutions further appear to define a boundary between two distinct nonlinear dynamical processes and may play significant roles in particle acceleration and transport.

ACKNOWLEDGMENTS

S.V.S. would like to thank her colleague T. Kamalam for her valuable suggestions.

- ¹A. E. Dubinov and D. Y. Kolotkov, *IEEE Trans. Plasma Sci.* **40**, 1429–1433 (2012).
- ²A. E. Dubinov and D. Y. Kolotkov, *Plasma Phys. Rep.* **38**, 909–912 (2012).
- ³F. Verheest, M. A. Hellberg, and I. Kourakis, *Phys. Plasmas* **20**, 082309 (2013).
- ⁴F. Verheest, M. A. Hellberg, and I. Kourakis, *Phys. Rev. E* **87**, 043107 (2013).
- ⁵M. A. Hellberg, T. K. Baluku, F. Verheest, and I. Kourakis, *J. Plasma Phys.* **79**, 1039–1043 (2013).
- ⁶O. R. Rufai, R. Bharuthram, S. V. Singh, and G. S. Lakhina, *Phys. Plasmas* **21**, 082304 (2014).
- ⁷O. R. Rufai, R. Bharuthram, S. V. Singh, and G. S. Lakhina, *Phys. Plasmas* **22**, 102305 (2015).
- ⁸S. V. Singh and G. S. Lakhina, *Commun. Nonlinear Sci. Numer. Simul.* **23**, 274–281 (2015).
- ⁹F. Verheest and M. A. Hellberg, *Phys. Plasmas* **22**, 012301 (2015).
- ¹⁰C. P. Olivier, S. K. Maharaj, and R. Bharuthram, *Phys. Plasmas* **22**, 082312 (2015).
- ¹¹A. Paul and A. Bandyopadhyay, *Astrophys. Space Sci.* **361**, 172 (2016).
- ¹²S. S. Varghese and S. S. Ghosh, *Phys. Plasmas* **23**, 082304 (2016).
- ¹³S. S. Ghosh and A. N. S. Iyengar, *Phys. Plasmas* **21**, 082104 (2014).
- ¹⁴S. V. Steffy and S. S. Ghosh, *Phys. Plasmas* **24**, 102111 (2017).
- ¹⁵R. Z. Sagdeev, in *Review of Plasma Physics*, edited by M. A. Lenovitch (Consultants Bureau, New York, 1966), Vol. 4, Page 23.
- ¹⁶F. Verheest, M. A. Hellberg, and I. Kourakis, *Phys. Plasmas* **20**, 012302 (2013).
- ¹⁷M. A. Hellberg, T. K. Baluku, and F. Verheest, *AIP Conf. Proc.* **1306**, 50 (2010).
- ¹⁸F. Verheest and C. P. Olivier, *Phys. Plasmas* **24**, 113708 (2017).
- ¹⁹R. B. White, B. D. Fried, and F. V. Coroniti, *Phys. Fluids* **15**, 1484 (1972).
- ²⁰S. S. Ghosh and A. N. S. Iyengar, *Phys. Plasmas* **4**, 3204–3210 (1997).
- ²¹L. Ostrovsky, E. Pelinovsky, V. Shrira, and Y. Stepanyants, *Chaos* **25**, 097620 (2015).
- ²²J. Engelbrecht, *Wave Motion* **14**, 85–92 (1991).
- ²³Z. Ehsan, N. L. Tsintsadze, J. Vranjes, and S. Poedts, *Phys. Plasmas* **16**, 053702 (2009).
- ²⁴A. Roy Chowdhury and G. Pakira, *Int. J. Theor. Phys.* **31**, 1335 (1992).
- ²⁵B. Kaur and S. Jana, *Pramana J. Phys.* **87**, 53 (2016).
- ²⁶D. Lu, Z. Li, H. Sang, and B. Xie, *Plasma Sci. Technol.* **19**, 035002 (2017).
- ²⁷M. Tribeche, S. Ghebache, K. Aoutou, and T. H. Zerguini, *Phys. Plasmas* **15**, 033702 (2008).
- ²⁸Y.-L. Li and Q.-L. Zha, *Commun. Theor. Phys.* **66**, 609 (2016).
- ²⁹T. Maytevarunyoo and B. A. Malomed, *J. Opt. Soc. Am. B* **25**, 1854–1863 (2008).
- ³⁰Y. Xiao-Yu, Z. Jiang-Bo, and D. Liang-Wei, *Chin. Phys. B* **20**, 034208 (2011).
- ³¹T. Alexander and Y. Kivshar, *Appl. Phys. B* **82**, 203–206 (2006).
- ³²Z. Zhi-Gang, *Commun. Theor. Phys.* **36**, 37 (2001).
- ³³A. Trochidis and B. Polyzos, *J. Appl. Phys.* **78**, 170–175 (1995).
- ³⁴C.-Q. Dai and F.-B. Yu, *Wave Motion* **51**, 52–59 (2014).
- ³⁵V. V. Smagin, A. P. Tankeyev, and M. A. Borich, *Phys. Met. Metallogr.* **108**, 425 (2009) [*Fiz. Met. Metallov.* **108**, 451–460 (2009)].
- ³⁶M. Vanitha and M. Daniel, *Phys. Rev. E* **85**, 041911 (2012).
- ³⁷X.-F. Pang and Y.-P. Feng, *Chem. Phys. Lett.* **373**, 392–401 (2003).
- ³⁸K. Ohmori, *J. High Energy Phys.* **2001**, 035.
- ³⁹B. B. Baizakov, A. Bouketir, A. Messikh, A. Benseghir, and B. A. Pumarov, *Int. J. Mod. Phys. B* **25**, 2427–2440 (2011).
- ⁴⁰S. Yanez-Pagans, D. Urzagasti, and Z. Oporto, *Phys. Rev. D* **96**, 083503 (2017).
- ⁴¹C. L. Emmott and A. J. Bray, *Phys. Rev. E* **54**, 4568–4575 (1996).
- ⁴²R. Grimshaw, D. Pelinovsky, E. Pelinovsky, and A. Slunyaev, *Chaos* **12**, 1070–1076 (2002).
- ⁴³S. Sundar, A. Das, V. Saxena, P. Kaw, and A. Sen, *Phys. Plasmas* **18**, 112112 (2011).
- ⁴⁴S. Abdoukary, A. Mohamadou, and T. Beda, *Commun. Nonlinear Sci. Numer. Simul.* **16**, 3525–3532 (2011).
- ⁴⁵T. Charitat and B. Fourcade, *Eur. Phys. J. B* **1**, 333–336 (1998).
- ⁴⁶F. Zhang, *Phys. Rev. E* **58**, 2558–2563 (1998).
- ⁴⁷N. S. Manton and H. Merabet, *Nonlinearity* **10**, 3 (1997).
- ⁴⁸R. Ali, A. Saha, and P. Chatterjee, *Indian J. Phys.* **91**, 689 (2017).